3 Biotech (2020) 10:467
https://doi.org/10.1007/s13205-020-02455-3

ORIGINAL ARTICLE

A histone H2A-derived antimicrobial peptide, Hipposin from mangrove whip ray, *Himantura walga*: Molecular and functional characterisation

P. P. Athira[1] · M. V. Anju[1] · V. V. Anooja[1] · K. Archana[1] · S. Neelima[1] · Philip Rosamma[1]

Received: 18 July 2020 / Accepted: 26 September 2020 / Published online: 9 October 2020

Abstract

Antimicrobial peptides (AMPs) are biologically dynamic molecules produced by all type of organisms as a fundamental component of their innate immune system. The present study deals with the identification of a histone H2A-derived antimicrobial peptide, Hipposin from mangrove whip ray, *Himantura walga*. A 243 base pair fragment encoding 81 amino acid residues amplified from complementary DNA was identified as Hipposin and termed as *Hw*-Hip. Homologous analysis showed that *Hw*-Hip belongs to the Histone H2A superfamily and shares sequence identity with other histone-derived AMPs from fishes. Phylogenetic analysis of *Hw*-Hip displayed clustering with the fish H2A histones. Secondary structure analysis showed the presence of three α-helices and four random coils with a prominent proline hinge. The physicochemical properties of *Hw*-Hip are in agreement with the properties of antimicrobial peptides. A 39-mer active peptide sequence was released by proteolytic cleavage in silico. Functional characterisation of active peptide in silico revealed antibacterial, anticancer and antibiofilm activities making *Hw*-Hip a promising candidate for further exploration.

Keywords Antimicrobial peptide · H2A derived · Ray fish · Hipposin · Histone

Introduction

Greatest threat in modern medicine is the emergence of drug-resistant microorganisms and lack of novel antibiotics to combat these pathogens. Golden age of antibiotics is reaching a culmination, and modern therapeutics have become essential to control bacterial infections (Lewies et al. 2019). Antimicrobial peptides (AMPs) are produced as first line of defense by all eukaryotic organisms with broad activity against microbes and cancer cells (Izadpanah and Gallo 2005). AMPs produced from precursor proteins by proteolytic cleavage are cationic with significant amount of hydrophobic residues (Boman 2003; Sruthy et al. 2019). Histones play an important role in the structural organisation of chromatin and also in post-translational modifications, crucial for gene regulation (Parseghian and Luhrs 2006; Poirier et al. 2014). Histones, a characteristic feature of eukaryotic organisms, participate in host defense by producing bioactive peptides through proteolytic cleavage.

In fishes, histone-derived peptides were found to be produced on exposure to Gram-negative bacteria or lipopolysaccharides (Katzenback 2015). Of these histone-derived peptides, the most dynamic and best described peptides are the histone H2A subunit (Birkemo et al. 2003; Cho et al. 2009; Koo et al. 2008; Park et al. 1996; Tsao et al. 2009). Abundance of the heat-resistant basic aminoacids (Arginine and lysine) at the N terminal makes histone H2A a potential precursor of AMPs (Cutrona et al. 2015). H2A-derived AMPs have been reported from both invertebrates and vertebrates. The invertebrate H2A peptides characterised are from *Chlamys farreri* (Li et al. 2007), *Haliotis discus discus* (De Zoysa et al. 2009), *Crassostrea madrasensis* (Sathyan et al. 2012a, b), *Litopenaeus vannamei* (Patat et al. 2004), *Macrobrachium rosenbergii* (Arockiaraj et al. 2013), *Scylla paramamosain* (Chen et al. 2015) and *Fenneropenaeus*

Electronic supplementary material The online version of this article (https://doi.org/10.1007/s13205-020-02455-3) contains supplementary material, which is available to authorized users.

✉ Philip Rosamma
rosammap@gmail.com

[1] Department of Marine Biology, Microbiology and Biochemistry, School of Marine Sciences, Cochin University of Science and Technology, Fine Arts Avenue, Kochi, Kerala 682016, India

indicus (Sruthy et al. 2019). H2A-derived AMPs have been reported from fishes (Vertebrates) viz., *Parasilurus asotus* (Park et al. 1998), *Salmo salar* (Richards et al. 2001), *Hippoglossus hippoglossus* (Birkemo et al. 2003), *Oncorhynchus mykiss* (Fernandes et al. 2002), *Tachysurus jella*, *Cynoglossus semifasciatus* (Chaithanya et al. 2013) and *Danio rerio* (Caccia et al. 2017). The temporal expression of parasin 1 in zebrafish from fertilised oocyte to mature adult indicated early expression of parasin 1 from ontogeny to adulthood and their inducibility by microbials.

AMPs reported from cartilaginous fishes include Himanturin from round whip ray *Himantura pastinacoides* (Sathyan et al. 2012a, b) and Harriottins, from sicklefin chimaera *Neoharriotta pinnata* (Sathyan et al. 2013). Buforin II is a well-characterised histone H2A-derived AMP from *Bufo gargarizans* (Kim et al. 1996; Park et al. 1996). The present study deals with the molecular characterisation and in silico evaluation of a histone H2A-derived AMP, Hipposin from mangrove whip ray, *Himantura walga*. The study will pave the way forward for exploration of H2A-derived peptides as therapeutants.

Materials and methods

Sample collection

Mangrove whip ray *Himantura walga* was collected from coastal waters of Cochin, Kerala, India, and was brought to the laboratory in live condition. Blood was collected from the gills and preserved in TRI reagent (Sigma) at − 20 °C till used.

RNA extraction and cDNA synthesis

Total RNA was isolated from the blood cells using TRI reagent (Sigma) as per the guidelines. RNA quality was tested on 0.8% agarose gel and also by A_{260}:A_{280} ratio measured using a Spectrophotometer (Hitachi U 2900). The RNAs having greater than 1.8 absorbance ratio were used for the study. The first strand cDNA was synthesised in a 20 µl volume reaction mix with 5 µg total RNA, 2 mmol/L dNTP, 20U of RNase inhibitor, 2 mmol/L oligo d(T20), 100U MMLV reverse transcriptase and 1 × RT buffer (New England Biolabs, USA). The reaction mix was incubated at 42 °C for 1 h followed by an inactivation step at 85 °C for 15 min.

PCR amplification and TA cloning

Amplification of Hipposin from cDNA was performed with hipposin primers (Forward 5′ATGTCCGGRMGMGGSAARAC 3′ and Reverse 5′GGGATGATGCGMGTCTTCTTGTT 3′). Beta actin was used as a reference gene to test the quality of the RNA (Forward 5′ATCATGTTCGAGACCTTCAACAC3′ and Reverse 5′CGATGGTGATGACCTGTCCGTC3′). The reaction was carried out in 25 µl reaction volume containing 1 × standard Taq buffer (10 mmol/L Tris–HCl, 50 mmol/L KCl, pH 8.3), 3.5 mmol/L $MgCl_2$, 200 mmol/L dNTPs, 0.4 mmol/L each primer and 1 U Taq DNA polymerase (New England Biolabs, USA). The PCR was carried out with an initial denaturation at 95 °C for 2 min followed by 35 cycles of 94 °C for 15 s, 60 °C for 30 s and 72 °C for 30 s and a final extension at 72 °C for 10 min. The amplicons were subjected to 1.5% agarose gel electrophoresis.

The purified PCR products were ligated into pGEM-T Easy clone vector and transformed into competent *Escherichia coli* DH5α cells (pGEM-T Easy TA Cloning Kit, Promega). Cells were grown in LB (Luria–Bertani) agar plates with IPTG, ampicillin and X-Gal at 37 °C for 14 h, and the recombinant clones were selected by blue/white screening followed by testing the inserts using gene-specific and vector-specific primers (T7 F and SP6 R). PCR condition consisted of 95 °C for 3 min followed by 35 cycles at 94 °C for 15 s, 57 °C for 30 s and 72 °C for 30 s and a final extension at 72 °C for 10 min. Amplicons were analysed on 1.5% agarose gel with ethidium bromide.

Plasmid isolation

Positive recombinant clones were subjected to plasmid isolation by GenElute HP Plasmid Miniprep Kit (Sigma). Isolated plasmids were analysed on 0.8% agarose gel. Gene-specific and vector-specific PCR amplifications were done to confirm the presence of insert. Sequencing of recombinant plasmid was done using ABI Prism 377 DNA sequencer (Applied Biosystem) at SciGenom, India.

Sequence analysis and molecular characterisation

The nucleotide sequence was processed using GeneTool, and the translation into amino acid sequence was done using the ExPASy translate (http://web.expasy.org/translate/). BLASTn and BLASTp algorithms were used for homology search. The physicochemical parameters such as molecular weight, extinction coefficient, isoelectric point, aliphatic index, instability index and grand average of hydropathicity (GRAVY) were studied using Expasy ProtParam (www.web.expasy.org/protparam). Boman index and wimley-white whole-residue hydrophobicity were predicted using APD3 tool (http://aps.unmc.edu/AP/main.php). Boman index is the protein-binding potential of the peptide and Wimley-white whole-residue hydrophobicity, the sum of whole-residue free energy of transfer of the peptide from water to POPC interface.

The architecture of the domain was analysed using SMART server (http://SMART.embl-heidelberg.de). Protein motif search was carried out using MOTIF (https://www.genome.jp/tools/motif). Pfam and SuperFamily database searches were done to assign the evolutionary relationships. Protein folding pattern recognition was carried out using PFP-FunD SeqE server (http://www.csbio.sjtu.edu.cn/bioinf/PFP-FunDSeqE). Coiled-coil conformation within the protein was identified with COILS server (https://embnet.vital-it.ch/software/COILS_form.html). Serine, tyrosine and threonine phosphorylation sites in the peptide were evaluated using NetPhos 3.1 server (http://www.cbs.dtu.dk/services/NetPhos).

RNA sequence was generated from the cDNA sequence of the peptide using biomodel server (http://biomodel.uah.es/en/lab/cybertory/analysis/trans.htm), and the RNA sequence was submitted to RNA Fold Server (http://rna.tbi.univie.ac.at/cgi-bin/RNAfold.cgi) for the visualisation of mRNA with minimum free energy (MFE). To determine the helical wheel, amino acid sequence was submitted in the heliquest server. Hydrophobicity of the peptide was predicted using the Kyte-Doolittle plot in ExPASy ProtScale server (http://web.expasy.org/protscale). ExPaSy NetSurfP (http://www.cbs.dtu.dk/services/NetSurfP) was used to analyse the accessible surface area of the protein.

Structure prediction

Peptide secondary structure prediction and analysis was done using PSIPRED (http://bioinf.cs.ucl.ac.uk/psipred/). Based on SWISS-MODEL homology analysis and template selection, the spatial structure was established with PyMOL (DeLano 2002). Stereochemical quality of the predicted model was analysed using Ramachandran plot constructed using PROCHECK (http://services.mbi.ucla.edu/PROCHECK/).

Phylogenetic analysis

Histone-derived AMP sequences were retrieved from the GenBank (NCBI), multiple alignment of the sequences was done using ClustalW and the Phylogenetic tree was constructed using MEGA 7 based on maximum likelihood (ML) method.

Subcellular localisation

Subcellular localisation is helpful for identifying the role of peptide at cellular level, and it was predicted for Hipposin *Hw*-Hip using CELLO analysis. The prediction is based on amino acid composition, physicochemical composition, N peptide composition and partitioned sequence composition (http://cello.life.nctu.edu.tw/). To identify the interacting components, STRING database (http://string-db.org/) was used.

Active peptide characterisation

Peptide cutter server (https://web.expasy.org/peptide_cutter/) was used to analyse the potential cleavage sites of the precursor histone, and the active peptide released was noted. Physicochemical properties of the active peptide were calculated using ProtParam and APD3 servers. The probability of expression of the protein in different expression systems was predicted using Codon Adaptation Index (CAI) Calculator (https://www.biologicscorp.com/tools/CAICalculator/#.Xo15x4gzbIU).

Functional prediction

The antimicrobial property of the active peptide *Hw*-Hip was predicted using Collection of Antimicrobial Peptides CAMP (http://www.camp.bicnirrh.res.in/) and iAMP-2L (http://www.jci-bioinfo.cn/iAMP-2L). Antifungal, antiviral, antiparasitic and anticancer activities were predicted using AntiFP (https://webs.iiitd.edu.in/ragHava/antifp/), AVPdb (http://crdd.osdd.net/servers/avpdb/), ParaPep (http://crdd.osdd.net/raghava/parapep/) and AntiCP (http://crdd.osdd.net/raghava/anticp/), respectively. Integrated data platform for food-derived bioactive peptides (BioPepDB) was also used to validate the result (http://bis.zju.edu.cn/biopepdbr/index.php?p=help). Antibiofilm activity of the peptide (http://ab-openlab.csir.res.in/abp/antibiofilm/) was predicted by dPABB and antiangiogenicity by AntiAngioPred (http://crdd.osdd.net/raghava/antiangiopred/). Cell-penetrating nature of *Hw*-Hip was checked on CellPPD (http://crdd.osdd.net/raghava/cellppd/). DNA-binding ability was analysed using DPbind (http://lcg.rit.albany.edu/dp-bind/), antitubercular activity by AtbPpred (http://thegleelab.org/AtbPpred) and toxicity prediction using ToxinPred tool (http://crdd.osdd.net/raghava/toxinpred/).

Results

A 243bp cDNA coding 81 amino acid was obtained from the gill mRNA transcripts of *H. Walga* (GenBank ID: MN563739). Nucleotide and amino acid BLAST analysis (Fig. 1) revealed that the peptide belonged to the Histone H2A-derived antimicrobial peptide family. BLASTn similarity searches indicated that *H. Walga* hipposin nucleotide sequence showed 95% similarity with *Himantura gerrardi* (KM605131.1), 90.95% similarity with *Pogona vitticeps* (XM020810498.1) and 90.50% similarity with *Ornithorhynchus anatinus* (XM001513380.3).

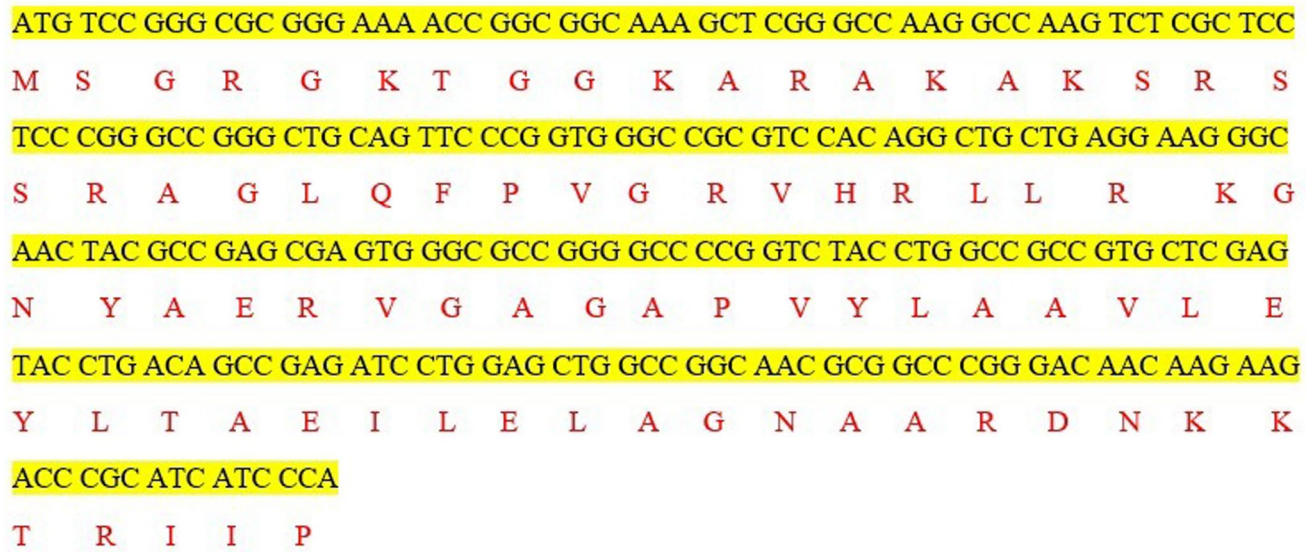

Fig. 1 Nucleotide and deduced amino acid sequence of histone-derived peptide Hipposin from mRNA transcripts of *Himantura walga*, *Hw*-Hip (GenBank ID:MN563739). The single-letter amino acid code is shown below the corresponding nucleotide sequences

Analysis by ProtParam predicted that the peptide is having a molecular weight of 8.66 kDa, theoretical isoelectric point (p*I*) of 11.26 and net charge of +12. Positive charge of the 81-mer *Hw*-Hip was mainly due to 17 cationic amino acids (Arg + Lys). Hipposin *Hw*-Hip was abundant with amino acids viz., Ala (16.0%), Arg (12.3%) and Gly (12.3%). The extinction coefficient and aliphatic index were calculated as 4470 and 42.15, respectively. Half-life of the peptide with respect to mammalian reticulocytes (in vitro), yeast (in vivo) and *E. coli* (in vivo) was identified as 30 h, > 20 h and > 10 h respectively. Instability index was calculated to be 42.15 indicating the peptide as unstable. GRAVY of the peptide was identified as -0.395. The APD3 predicted the *Hw*-Hip as an AMP with a boman index (Protein-binding potential) of 2.01 kcal/mol and wimley whole residue hydrophobicity as 21.71 kcal/mol.

SMART domain prediction and motif search by MOTIF server (Genome net) identified the presence of a histone H2A domain and two functional motifs, i.e. core histone motif and histone-like transcription factor motif. Pfam server and SuperFamily server analysis indicated that *Hw*-Hip comes under nucleosome core histone family and histone superfamily. Fold pattern recognition by PFP-FunDSeqE tool revealed the presence of three DNA binding helical folds, indicating its DNA interacting ability. COILS server analysis showed that there is no coil conformation in *Hw*-Hip.

Phosphorylation sites were predicted using NetPhos 3 tool identified four serine phosphorylations in *Hw*-Hip at 2, 17, 19 and 20th positions. In addition, three possible threonine phosphorylation sites at positions 7, 60, 77 and one tyrosine phosphorylation site at position 40 were also predicted. Stem loops are the common elements of RNA structure. The multiloop, internal loop, hairpin loop and bulges of the *Hw*-Hip RNA play significant role in structural stability besides providing recognition sites for RNA-binding proteins (Fig. 2). The mRNA structure predicted has − 106.20 kcal/mol minimum free energy (MFE), indicating its structural stability. The helical wheel server showed that *Hw*-Hip is an alpha helical linear molecule with hydrophilic and hydrophobic residues arranged in opposing sides (Fig. 3). Kyte-Doolittle hydrophobicity plot of *Hw*-Hip confirmed the presence of hydrophobic amino acids located at R^{20}AGLQFPVGRV^{30} and E^{40}RVGAGAPVYLAAVLEYLTAEILELAGNAA^{70} (Fig. 4). The relative surface accessibility of *Hw*-Hip identified by NetSurfP showed a mixture of exposed and buried amino acid residues at 25% threshold level.

Secondary structure analysis of *Hw*-Hip indicated α-helical structure with random coils (Fig. 5). Spatial 3D structure prediction of *Hw*-Hip by homology modelling using SWISS MODEL showed the occurrence of alternative α helical and random coil with proline hinge region (Fig. 6). Crystal structure of a core histone octamer (6k1k.1.G) was selected as template. N-terminal and C-terminal region are coiled in structure, and thereby *Hw*-Hip has a helix-hinge-helix structure. Presence of proline at position 26 with a proline hinge was characteristic feature of *Hw*-Hip. Ramachandran plot (Fig. 7) showed 85.9% residues in the most favoured regions, 7.8% in additional allowed region, 4.7% in disallowed regions and 1.6% in generously allowed regions. Residue in the generously allowed region (~ b) was identified as lysine, and in disallowed region as alanine, lysine and arginine.

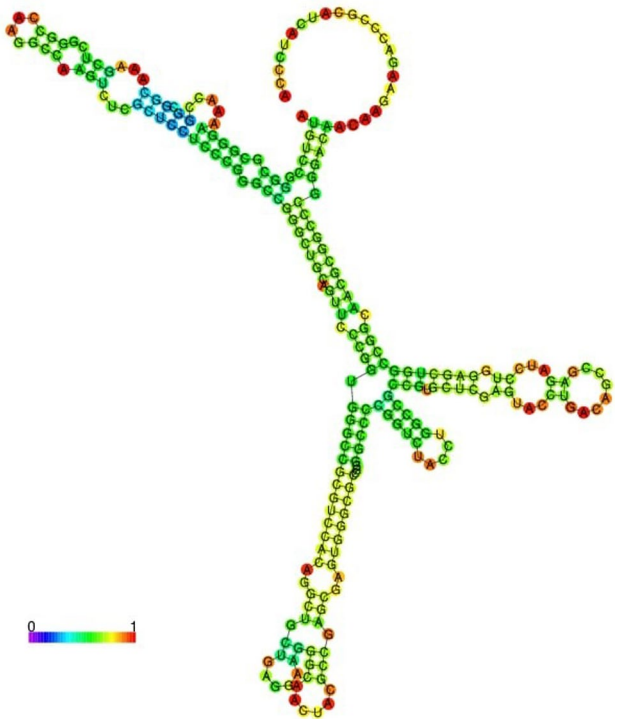

Fig. 2 Predicted mRNA structure of *Himantura walga* Hipposin, *Hw*-Hip, drawn using RNA-fold server with minimal free energy prediction. Predicted RNA structure is well structured and stable

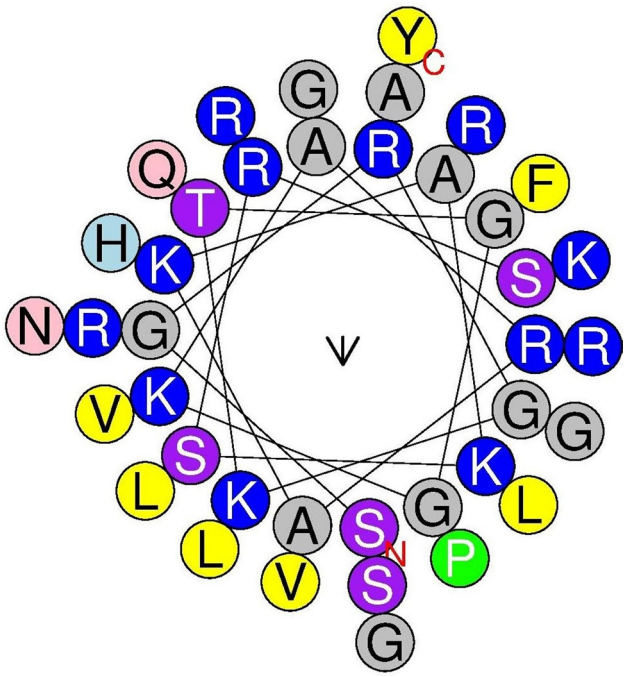

Fig. 3 The helical wheel diagram of *Hw*-Hip predicted using Heliquest online tool. The structure was built to identify the amphipathicity of the peptide. Hydrophilic and hydrophobic amino acids are arranged on the opposite phases of peptide

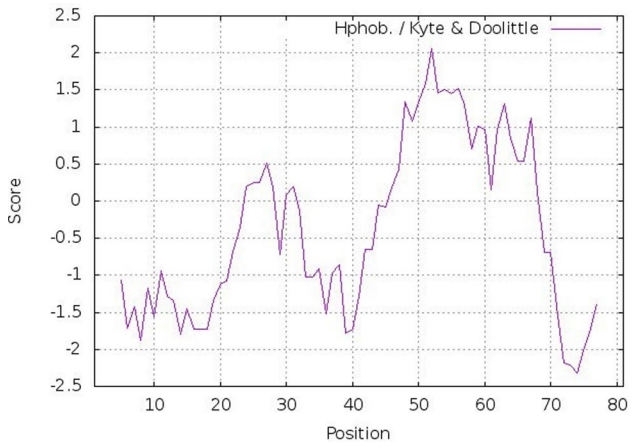

Fig. 4 Kyte-Doolittle plot showing hydrophobicity of *Hw*-Hip. The peaks above the score (0.0) indicate the hydrophobic nature of the predicted protein. Positive peaks showing predicted hydrophobic regions

The plot showed that the glycine and proline were found in the allowed and favoured regions. The Ramachandran plot shows a tight grouping of − 60° phi and − 45° to − 50° psi values for *Hw*-Hip confirming right-handed α helix formation.

Subcellular localisation of *Hw*-Hip was predicted as nuclear based on amino acid composition, physicochemical properties, N-peptide composition and partitioned sequence composition with the reliability values as 0.74, 0.85, 0.79 and 0.65 respectively. Protein–protein interactions and functional protein association network analysis were used to understand the metabolic roles of hipposin, which is visualised as nodes and arcs (Fig. 8). Eleven proteins were found putatively associated with *Hw*-Hip. Histone H2A-like protein from *Larimichthys crocea* (EH28_07767) was used as template to analyse protein–protein interaction, and it was found that H2A, H2B, H3, H4 (Core histone) proteins and H1 (Linker histone) protein are interacting with *Hw*-Hip protein.

The amino acid sequence of *Hw*-Hip was aligned with other histone H2A relatives (Fig. 9) and was found to have significant similarity with himanturin and teleostin. Threonine at the 16th position of both hipposin and himanturin have been replaced by serine in *Hw*-Hip. It is observed that the 7th amino acid of *Hw*-Hip from its N-terminus, the hydrophilic threonine/glutamine is same for all other vertebrate H2A-derived AMPs; but the position is vacant or there is a gap for invertebrate H2A-derived AMPs. Both glutamine and threonine belong to uncharged aminoacids and thereby this variation do not affect the charge of the peptides. The N-terminal region of all H2A-derived AMPs is rich in basic amino acids (arginine and lysine), and the amino acid positions 18-41 of *Hw*-Hip are found to be highly conserved.

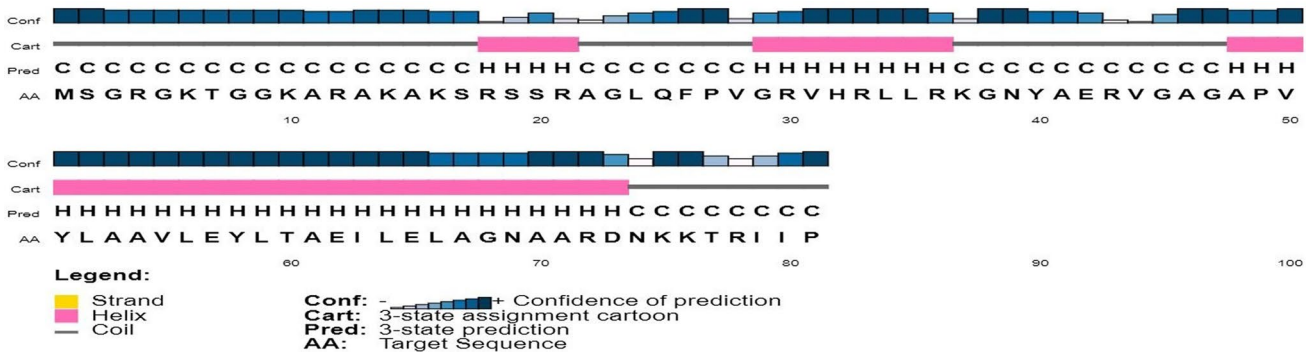

Fig. 5 Secondary structure of *Hw*-Hip predicted using PSIPRED server. The α-helix region is shown in pink-coloured cylinders and the coiled region is shown in black lines. *Hw*-Hip structure indicated α-helical structure with random coils

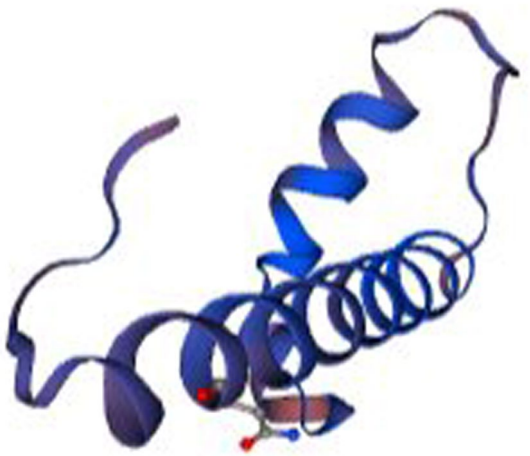

Fig. 6 Structural model of *Hw*-Hip created with the PyMol software using the pdb data generated by SWISS MODEL server. Model showing alternative α helical and random coil with proline hinge region

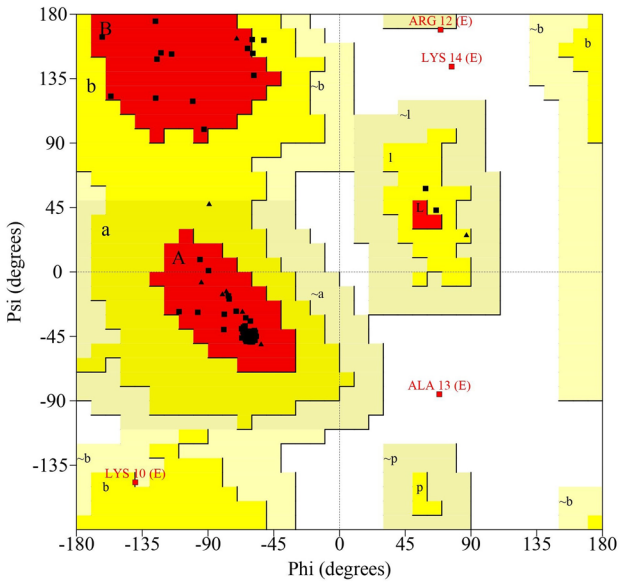

Fig. 7 Ramachandran plot analysis of phi-psi graph for the predicted 3D structure of *Hw*-Hip as computed by PROCHECK program. The areas A, B and L represent the most favoured region, whereas a, b, l and p mark the additional allowed regions. The ~a, ~b, ~l and ~p areas designate generously allowed regions. The area that does not fall to any of these categories is considered as disallowed region

Phylogenetic tree based on the amino acid sequences of histone H2A grouped into two main clades, invertebrate H2A peptides and vertebrate H2A peptides (Fig. 10). The vertebrate group further grouped into fishes, amphibians, reptiles, birds and mammals. Invertebrate cluster includes H2A-derived AMPs from crustaceans and molluscs. *Hw*-Hip aligned with fish clade, indicating its close resemblance with chondrichthyes while Osteichthyes formed a separate group. H2A sequence from *Neoharriotta pinnata* was found to be positioned between invertebrate and vertebrate group. In the H2A sequences of reptiles and birds, an overlap was noticed.

Peptide cutter analysis revealed that *Hw*-Hip has cleavage sites for proteolytic enzymes viz, chymotrypsin, pepsin, proteinase K and thermolysin. Chymotrypsin and pepsin (pH > 2) digestion released a 39-mer active peptide sequence (S^{2}GRGKTGGKARAKAKSRSSRAGLQFPVGR VHRLLRKGNY^{39}) from histone precursor molecule. Furthermore, the *Hw*-Hip with + 12 charge and boman index of 3.22 kcal/mol was found to possess antimicrobial property. APD3 analysis showed the presence of 10 hydrophobic residues in the mature peptide recording a GRAVY of – 1.05, indicating a prominent interaction with the microbial membrane and thereby antimicrobial property. The codon adaptation index (CAI) indicates the likely success of heterologous gene expression. The estimated CAI of the peptide was predicted to be 0.58 for *Escherichia coli*, 0.44 for *Pichia pastoris*, 0.43 for *Saccharomyces cerevisiae*, 0.76 for *Spodoptera frugiperda* and 0.88 for *Cricetulus griseus* expression systems. All these results denote that *Hw*-Hip can be expressed in all these expression systems for further exploration.

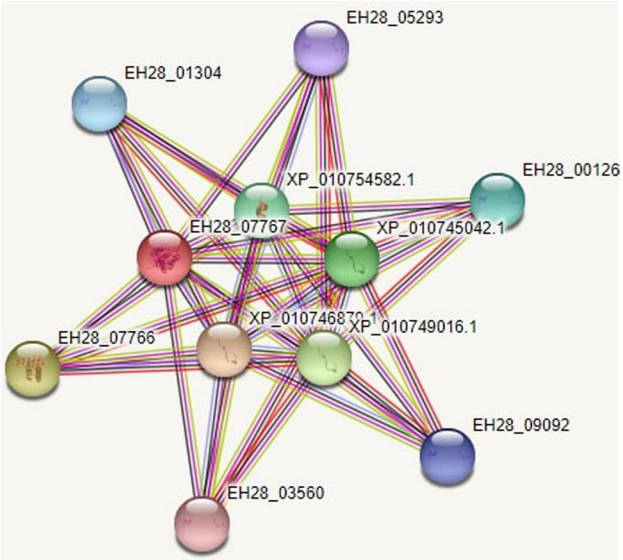

Fig. 8 Functional protein association networks of *Hw*-Hip using STRING software. Protein– protein interaction visualised using histone H2A-like protein *Larimichthys crocea* (EH28_07767) database: EH28_07767 (Histone H2A-like), EH28_05293 (Histone H2B 1/2-like), XP_010745042.1 (Histone H3.3-like), XP_010754582.1(Histone H4 like), EH28_01304 (Histone H2B 1/2-like), EH28_00126 (Histone H2B 1/2-like), EH28_07766 (Histone H2B 3), EH28_09092(Histone H2B 1/2-like), XP_010749016.1 (Histone H3-like), EH28_03560 (Histone H2B 1/2-like), XP_010746879.1(Histone H4 like)

Peptide *Hw*-Hip was confirmed as antimicrobial peptide by CAMP analysis with an AMP probability of 0.940. *Hw*-Hip was found to have antibacterial and anticancer activity by iAMP-2L and BioPepDB prediction, respectively. AntiCP identified *Hw*-Hip as anticancer peptide with an average SVM score of 0.73. AntiAngioPred predicted that *Hw*-Hip is an antiangiogenic peptide indicating its potential to inhibit the cancer progression. It was observed that *Hw*-Hip has no antifungal, antiviral and antiparasitic activity. The dPABBs analysis identifies antibiofilm peptides based on total amino acid composition and positional preference of specific amino acid residues and the *Hw*-Hip was found to have antibiofilm property. A characteristic feature of histone-derived AMPs is its DNA binding ability. *Hw*-Hip is a cell penetrating peptide with DNA binding propensity; 77% of the residues of the 39-mer peptide binding potential fell in the range of 0.540 to 1 which suggested that the peptide has DNA binding property. *Hw*-Hip is an anti-tubercular peptide with 0.721 probability as per AntiTB_MD prediction model suggesting its antimycobacterial activity. ToxinPred server identified *Hw*-Hip as a non-toxic peptide. These functional characterisations revealed that *Hw*-Hip is a promising lead molecule for drug development.

Discussion

Histone proteins play a significant role in the regulation of transcription, replication and DNA packaging. These proteins form the basic building blocks of chromatin structure with the four core histone proteins: i.e., H2A, H2B, H3 and H4 with DNA forming the nucleosome along with H1/H5 the linker histones (Chen et al. 2015). The antimicrobial properties of histone and histone-derived sequences have been characterised from various vertebrate species; however, there is only one previous report from ray fish (Sathyan et al. 2012a, b).The present study deals with the identification and characterisation of a hipposin from histone H2A of a cartilaginous fish *H. walga*.

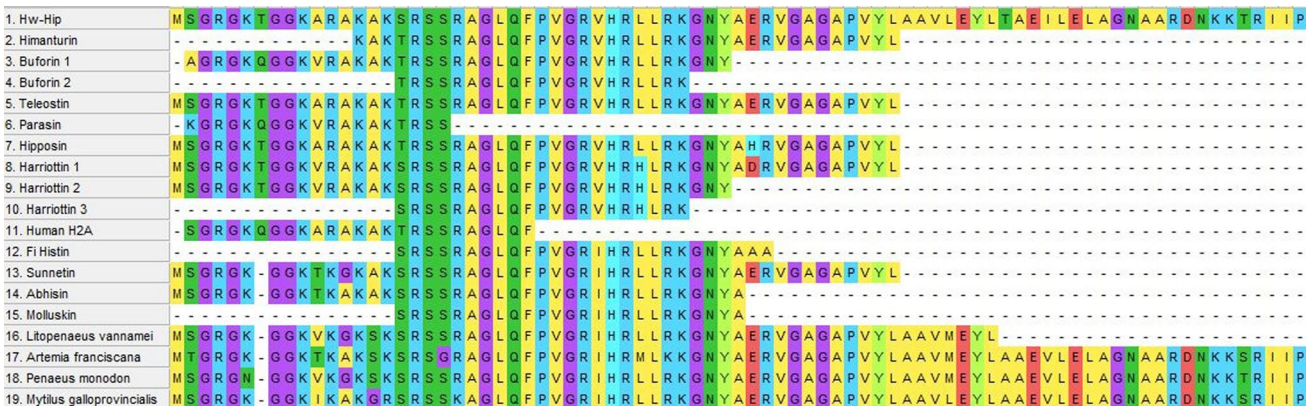

Fig. 9 Multiple alignment of amino acid sequence of the *Hw*-Hip with other vertebrate and invertebrate H2A sequences obtained using BioEdit; Himanturin (*Himantura pastinacoides*), Buforin (*Bufo bufo gargarizans*), Teleostin (*Tachysurus jella* and *Cynoglossus semifasciatus*), Parasin (*Parasilurus asotus*), Hipposin (*Hippoglossus hippoglossus*), Harriotins (*Neoharriotta pinnata*), Human H2A, *Fi* Histin (*Fenneropenaeus indicus*), Sunettin (*Sunetta scripta),* Abhisin (*Haliotis discus*), Molluskin (*Crassostrea madrasensis*), *Litopenaeus vannamei* H2A, *Artemia franciscana* H2A, *Penaeus monodon* H2A and *Mytilus galloprovincialis* H2A

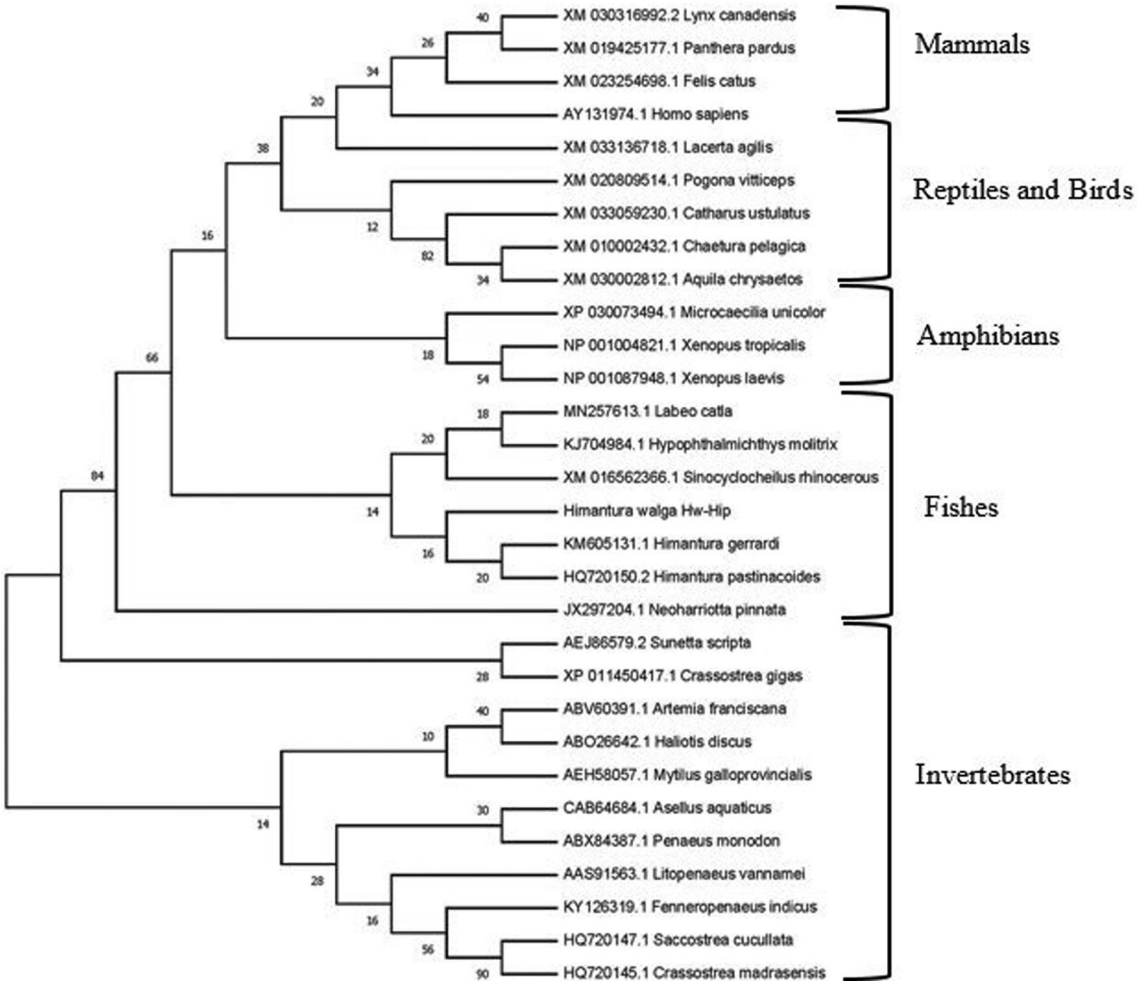

Fig. 10 Bootstrapped maximum likelihood tree obtained using MEGA version 7 illustrating relationships between the amino acid sequence of *Hw*-Hip to the amino acid sequences of previously reported histone H2A from different organisms

Histone H2A-derived antimicrobial peptides are produced by the proteolytic cleavage of a precursor molecule. Cleavage of histone H2A from *Bufo gargarizans* at position $Y^{39} - A^{40}$ by pepsin released a peptide, buforin I from precursor histone (Kim et al. 2000). Cleavage of S^{19}-R^{20} bond of histone H2A from *Parasilurus asotus* by cathepsin D released an active peptide, parasin I (Cho et al. 2002). Outer membrane proteases of bacteria induce the production of histone-derived antimicrobial peptides, suggesting an infection-induced production of the peptides (Kawasaki et al. 2008). To understand the cleavage sites on histone H2A of *H. walga*, Peptide Cutter tool was used. A 39-mer active peptide was released by chymotrypsin and pepsin (pH > 2). All these results suggest that histone-derived AMPs are produced by the cleavage of a precursor protein molecule, histone. Cleavage of the precursor histone molecule depends upon the type of pathogen/antigen involved in infection. Bacterial infection and AMP production is a co-evolution process in which novel AMPs are produced as a result of exposure to novel epitopes of antigens.

Hw-Hip has been characterised as positively charged, amphipathic molecule with 8.66 kDa molecular weight and 11.26 theoretical isoelectric point. It has all the histone H2A distinct features including H2A signature motif and 95% nucleotide sequence similarity with previously reported histone-derived AMPs. The helical wheel diagram showed that the polar and non-polar amino acids are arranged on opposing face along the amphipathic helix. *Hw*-Hip contains 61% α-helical region and 39% coiled region. Boman (2003) stated that proteins having more α -helix regions display higher antimicrobial activity. Proline act as a hinge between N-terminal and C-terminal region (Yi et al. 1996), which is essential for the successful translocation of peptide into the cell (Kobayashi et al. 2000; Park et al. 2000). The antimicrobial property of *Hw*-Hip is mainly due to the ability of proline hinge to promote peptide translocation and

interaction with DNA/RNA. The predicted physicochemical characteristics of *Hw*-Hip showed it to be a potential antimicrobial peptide.

Phosphorylation is a post-translational modification in histones and the *Hw*-Hip showed serine phosphorylation at four sites, threonine phosphorylation at three sites and tyrosine phosphorylation at one site. The extent of phosphorylation in histone influences its potential to interconnect with DNA, modulating its susceptibility to proteolytic degradation (Hill et al. 1991; Morin et al. 2000). *Hw*-Hip, the H2A-derived AMP, was found interacting with other H2B, H3 and H4 (Core histones) and H1 (linker histone) proteins. Lysine-rich histone (H2A, H2B, and H1) proteins have nucleic acid binding mode of action, and arginine-rich histones (H3 and H4) have membrane disruption mode of action. All these histone proteins act synergistically to effectively kill the target pathogen (Tagai et al. 2011).

Hw-Hip when aligned with previously reported H2A-derived peptides showed many conserved residues within the sequences. The twenty eighth amino acid from N-terminus of *Hw*-Hip is valine, a characteristic feature of vertebrate H2A-derived peptide which is replaced by isoleucine in all invertebrates. Interchange of isoleucine and valine do not change the charge of the peptide as they are hydrophobic and neutral (Sathyan et al. 2012a, b). The arginine and lysine rich N-terminus of H2A sequence that serve as nuclear localisation signal signifies the nucleic acid interacting mode of action of histone H2A-derived peptides (Cutrona et al. 2015).

Sequence homology between proteins is defined in terms of shared ancestry. The phylogenetic tree of H2A histones formed two separate clusters of vertebrates and invertebrates. *Hw*-Hip is evolutionarily more related to H2A-derived peptides of chondrichthyes fishes. *N. pinnata* represents holocephalan fishes which are divergent offshoot from primitive elasmobranch stem. *N. pinnata* H2A-derived peptide occupies a position between vertebrate and invertebrate groups (Sathyan et al. 2013). Overlap in the H2A sequence of reptiles and birds might be due to slow rate of evolution of histone-derived peptides (Sathyan et al. 2012a, b) and orthologous nature of sequences. All these modulations during the course of evolution are the driving force to adapt in different environments.

Histone-derived peptides display diverse mode of actions like permeabilisation of bacterial membrane, penetration into the cell followed by nucleic acid binding and lipopolysaccharide (LPS) binding resulting in neutralising the LPS toxicity (Kawasaki et al. 2008). Hipposin is one among the most potent antimicrobial peptides discovered to date (Birkemo et al. 2003). In silico analysis showed that *Hw*-Hip is a potent molecule having antibacterial, anticancer and antibiofilm activities. Cationic *Hw*-Hip interacting with anionic target membrane facilitates the lysis of bacterial cells by cell membrane disruption. Helical property of the peptide plays an important role in regulating the antimicrobial activity (Koo et al. 2008). Sruthy et al. (2019) observed LPS binding activity of an H2A-derived AMP, histin from *F. indicus* and reported that the α-helical peptide could attach to the bacterial membrane segregating hydrophilic and hydrophobic amino acids and allowing the interaction with the phospholipid bilayer of pathogen resulting in the membrane rupture and leakage of contents. Translocation of cell penetrating peptide is mainly promoted by increased arginine content or other guanidinium groups (Cutrona et al. 2015). Bactericidal mechanism of buforin II was reported as membrane translocation and DNA binding (Pavia et al. 2012). *Hw*-Hip showed a prominent DNA interaction property with 77% binding propensity. Thus, based on the properties like the α-helicity, cell penetrating ability, presence of proline hinge, physicochemical parameters, arginine content, DNA binding ability and sequence similarity with well characterised H2A-derived AMPs, it could be inferred that *Hw*-hip is a potential antimicrobial peptide.

Peptides are considered as an alternative drug for conventional chemotherapeutic agents. These peptides have several advantages over currently used anticancer therapeutics, such as cancer cell selective toxicity, bypassing multidrug-resistance mechanism and combination therapy additive effects (Lee et al. 2008; Papo and Shai 2005).The buforin IIb specifically targets the cancer cells via interacting with cell membrane phosphatidylserine, gangliosides and heparin sulphate. The peptide is internalised without causing membrane damage and mediates the intrinsic pathway of cancer cell apoptosis (Lee et al. 2008). Histone-derived peptide *Fi*-Histin causes the release of cytochrome C from mitochondria and thereby upregulating caspase 3 and 9, leading to apoptosis of cancer cells (Sruthy et al. 2019). AntiCP identified *Hw*-Hip as an anticancer peptide with a prominent SVM score. The *Hw*-Hip is assumed to have similar mode of anticancer action by virtue of its structure and sequence similarity. Tumours induce angiogenesis (Blood vessel growth) by secreting different proteins and growth factors (McDougall et al. 2006; Spill et al. 2015). Hypoxia inducible factor 1 alpha (HIF 1α) is an important gene involved in angiogenesis. Post-translational modification such as histone acetylation and histone deacetylation modulates HIF-1α expression (Deng et al. 2020). In silico analysis proved that *Hw*-Hip is having antiangiogenic property which might be due to its histone based origin. This opens the possibility to make use of anticancer properties of the peptide in cancer healthcare.

Microbes in biofilms are more resistant to antibiotics than freely suspended planktonic forms. The major biofilm forming pathogens are *Staphylococcus aureus*, *Escherichia coli* and *Pseudomonas aeruginosa* (Jodoin and Hincke 2018). Total histones (H1, H2A, H2B, H3, H4 and H5) from chicken erythrocytes were found to exhibit

antibiofilm activity (Rose-Martel and Hincke 2014). However, among histone-derived peptides, only H5-derived peptides showed antibiofilm activity against methicillin-resistant and methicillin-sensitive *S. aureus* (Rose-Martel et al. 2017). The antibiofilm mechanisms include decreasing the membrane potential of microbes in the biofilm (Okuda et al. 2013), interruption of the bacterial cell signalling system (Habets and Brockhurst 2012), degradation of the polysaccharide and biofilm matrix (Ansari et al. 2017), inhibition of the alarmone system affecting the bacterial responses (Pletzer et al. 2016) and downregulation of genes responsible for binding protein transportation and biofilm formation (Rohde et al. 2010). dPABBs analysis revealed that *Hw*-Hip, the H2A-derived antimicrobial peptide possess antibiofilm property. Antibiofilm peptides are rich with cationic (K, H, R) and polar (D,E, R, K, Q, N) amino acids. In *Hw*-Hip, the high content of cationic and polar residues facilitate the access to the aqueous extracellular polymeric substances (EPS) of biofilm (Sharma et al. 2016) effecting the antibiofilm activity.

Conclusion

An antimicrobial peptide was identified from the histone H2A of *H. Walga* and was termed as *Hw*-Hip. Sequence similarity of *Hw*-Hip to previously reported histone H2A-derived AMPs along with physicochemical and functional properties strongly indicate *Hw*-Hip to be an antimicrobial, anticancer and antibiofilm peptide with potential applications. This study also illustrates the importance of H2A-derived AMP in the innate immune system in chondrichthyes. The need based cleavage of these histone proteins is highly significant in defense. The type of infection or physiological impairment (malignancy) plays a significant role in the determination of the position of cleavage of the histone proteins and the resultant bioactive peptides for immediate action in the host. So the histones are a treasure house of therapeutic peptides which can be harnessed for health management in aquaculture or medicine.

Acknowledgements The authors are grateful to the Director, Centre for Marine Living Resources and Ecology (CMLRE) and Ministry of Earth Sciences (MoES), Govt. of India for the research grant (MoES/10-MLR/01/2012) and scientific support for the work. The authors also thank Cochin University of Science and Technology for providing necessary facilities to carry out this work. The first author gratefully acknowledges CSIR (Council of Scientific & Industrial Research) for the award of a fellowship.

Author contributions Athira P P carried out the experiment with the support from Anju M V, Anooja V V, Archana K and Neelima S. Athira P P wrote the manuscript. Rosamma Philip supervised the work and corrected the manuscript.

Compliance with Ethical Standards

Conflict of interest Authors declare that there is no conflict of interest.

Research involving human and animal participants This article does not contain any study that requires ethical approval.

References

Ansari JM, Abraham NM, Massaro J, Murphy K, Smith-Carpenter J, Fikrig E (2017) Anti-biofilm activity of a self-aggregating peptide against *Streptococcus* mutans. Front Microbiol 8:488

Arockiaraj J, Gnanam AJ, Kumaresan V, Palanisamy R, Bhatt P, Thirumalai MK, Kasi M (2013) An unconventional antimicrobial protein histone from freshwater prawn *Macrobrachium rosenbergii*: analysis of immune properties. Fish shellfish immun 35:1511–1522

Birkemo GA, Lüders T, Andersen Ø, Nes IF, Nissen-Meyer J (2003) Hipposin, a histone-derived antimicrobial peptide in Atlantic halibut (*Hippoglossus hippoglossus* L.). Biochim Biophys Acta 1646:207–215

Boman HG (2003) Antibacterial peptides: basic facts and emerging concepts. J Intern Med 254:197–215

Caccia E, Agnello M, Ceci M, Strickler Dinglasan P, Vasta GR, Romano N (2017) Antimicrobial peptides are expressed during early development of zebrafish (*Danio rerio*) and are inducible by immune challenge. Fishes 2:20

Chaithanya ER, Philip R, Sathyan N, Anil Kumar PR (2013) Molecular characterization and phylogenetic analysis of a histone-derived antimicrobial peptide teleostin from the marine teleost fishes. *Tachysurus jella* and *Cynoglossus semifasciatus*. ISRN Mol, Biol

Chen B, Fan DQ, Zhu KX, Shan ZG, Chen FY, Hou L, Wang KJ (2015) Mechanism study on a new antimicrobial peptide Sphistin derived from the N-terminus of crab histone H2A identified in haemolymphs of *Scylla paramamosain*. Fish shellfish Immun 47:833–846

Cho JH, Park IY, Kim HS, Lee WT, Kim MS, Kim SC (2002) Cathepsin D produces antimicrobial peptide parasin I from histone H2A in the skin mucosa of fish. FASEB J 16:429–431

Cho JH, Sung BH, Kim SC (2009) Buforins: histone H2A-derived antimicrobial peptides from toad stomach. BBA-Biomembranes 1788:1564–1569

Cutrona KJ, Kaufman BA, Figueroa DM, Elmore DE (2015) Role of arginine and lysine in the antimicrobial mechanism of histone-derived antimicrobial peptides. FEBS Lett 589:3915–3920

De Zoysa M, Nikapitiya C, Whang I, Lee JS, Lee J (2009) Abhisin: a potential antimicrobial peptide derived from histone H2A of disk abalone (*Haliotis discus discus*). Fish shellfish Immun 27:639–646

DeLano WL (2002) Pymol: an open-source molecular graphics tool. CCP4 Newsletter Protein Crystallogr 40:82–92

Deng B, Luo Q, Halim A, Liu Q, Zhang B, Song G (2020) The antiangiogenesis role of histone deacetylase inhibitors: their potential application to tumour therapy and tissue repair. DNA Cell Biol 39:167–176

Fernandes JM, Kemp GD, Molle MG, Smith VJ (2002) Anti-microbial properties of histone H2A from skin secretions of rainbow trout, *Oncorhynchus mykiss*. Biochem J 368:611–620

Habets MG, Brockhurst MA (2012) Therapeutic antimicrobial peptides may compromise natural immunity. Biol Lett 8:416–418

Hill CS, Rimmer JM, Green BN, Finch JT, Thomas JO (1991) Histone-DNA interactions and their modulation by phosphorylation of-Ser-Pro-X-Lys/Arg-motifs. EMBO J 10:1939–1948

Izadpanah A, Gallo RL (2005) Antimicrobial peptides. J Am Acad Dermatol 52:381–390
Jodoin J, Hincke MT (2018) Histone H5 is a potent antimicrobial agent and a template for novel antimicrobial peptides. Sci Rep 8:1–15
Katzenback BA (2015) Antimicrobial peptides as mediators of innate immunity in teleosts. Biology 4:607–639
Kawasaki H, Iwamuro S (2008) Potential roles of histones in host defense as antimicrobial agents. Infect Disord Drug Targets 8:195–205
Kawasaki H, Koyama T, Conlon JM, Yamakura F, Iwamuro S (2008) Antimicrobial action of histone H2B in *Escherichia coli*: evidence for membrane translocation and DNA-binding of a histone H2B fragment after proteolytic cleavage by outer membrane proteinase. T Biochim 90:1693–1702
Kim HS, Park CB, Kim MS, Kim SC (1996) cDNA cloning and characterization of buforin I, an antimicrobial peptide: a cleavage product of histone H2A. Biochem Biophys Res Commun 229:381–387
Kim HS, Yoon H, Minn I, Park CB, Lee WT, Zasloff M, Kim SC (2000) Pepsin-mediated processing of the cytoplasmic histone H2A to strong antimicrobial peptide buforin I. J Immunol 165:3268–3274
Kobayashi S, Takeshima K, Park CB, Kim SC, Matsuzaki K (2000) Interactions of the novel antimicrobial peptide buforinII with lipid bilayers: proline as a translocation promoting factor. Biochemistry US 39:8648–8654
Koo YS, Kim JM, Park IY, Yu BJ, Jang SA, Kim KS, Kim SC (2008) Structure–activity relations of parasin I, a histone H2A-derived antimicrobial peptide. Peptides 29:1102–1108
Lee HS, Park CB, Kim JM, Jang SA, Park IY, Kim MS, Kim SC (2008) Mechanism of anticancer activity of buforin IIb, a histone H2A-derived peptide. Cancer Lett 271:47–55
Lewies A, Du Plessis LH, Wentzel JF (2019) Antimicrobial peptides: the Achilles heel of antibiotic resistance. Probiot Antimicrob Proteins 11:370–381
Li C, Song L, Zhao J, Zhu L, Zou H, Zhang H, Cai Z (2007) Preliminary study on a potential antibacterial peptide derived from histone H2A in hemocytes of scallop *Chlamys farreri*. Fish shellfish Immun 22:663–672
McDougall SR, Anderson AR, Chaplain MA (2006) Mathematical modelling of dynamic adaptive tumour-induced angiogenesis: clinical implications and therapeutic targeting strategies.J. Theor Biol 241:564–589
Morin V, Acuña P, Díaz F, Inostroza D, Martinez J, Montecino M, Imschenetzky M (2000) Phosphorylation protects sperm-specific histones H1 and H2B from proteolysis after fertilization. J Cell Biochem 76:173–180
Okuda KI, Zendo T, Sugimoto S, Iwase T, Tajima A, Yamada S, Mizunoe Y (2013) Effects of bacteriocins on methicillin-resistant *Staphylococcus aureus* biofilm. Antimicrob Agents Chemother 57:5572–5579
Papo N, Shai Y (2005) Host defense peptides as new weapons in cancer treatment. Cell Mol Life Sci 62:784–790
Park CB, Kim MS, Kim SC (1996) A novel antimicrobial peptide *from Bufo bufo gargarizans*. Biochem Biophys Res Commun 218:408–413
Park IY, Park CB, Kim MS, Kim SC (1998) Parasin I, an antimicrobial peptide derived from histone H2A in the catfish, *Parasilurus asotus*. FEBS Lett 437:258–262
Park CB, Yi KS, Matsuzaki K, Kim MS, Kim SC (2000) Structure–activity analysis of buforin II, a histone H2A-derived antimicrobial peptide: the proline hinge is responsible for the cell-penetrating ability of buforin II. Proc Natl Acad Sci USA 97:8245–8250
Parseghian MH, Luhrs KA (2006) Beyond the walls of the nucleus: the role of histones in cellular signalling and innate immunity. Biochem Cell Biol 84:589–595
Patat SA, Carnegie RB, Kingsbury C, Gross PS, Chapman R, Schey KL (2004) Antimicrobial activity of histones from hemocytes of the Pacific white shrimp. Eur J Biochem 271:4825–4833
Pavia KE, Spinella SA, Elmore DE (2012) Novel histone-derived antimicrobial peptides use different antimicrobial mechanisms. BBA-Biomembranes 1818:869–876
Pletzer D, Coleman SR, Hancock RE (2016) Anti-biofilm peptides as a new weapon in antimicrobial warfare. Curr Opin Microbiol 33:35–40
Poirier AC, Schmitt P, Rosa RD, Vanhove AS, Kieffer-Jaquinod S, Rubio TP, Destoumieux-Garzón D (2014) Antimicrobial Histones and DNA Traps in Invertebrate Immunity evidences in *Crassostrea gigas*. J Biol 289:24821–24831
Richards RC, O'Neil DB, Thibault P, Ewart KV (2001) Histone H1: an antimicrobial protein of Atlantic salmon (*Salmo salar*). Biochem Biophys Res Commun 284:549–555
Rohde H, Frankenberger S, Zähringer U, Mack D (2010) Structure, function and contribution of polysaccharide intercellular adhesin (PIA) to Staphylococcus epidermidis biofilm formation and pathogenesis of biomaterial-associated infections. Eur J Cell Biol 89:103–111
Rose-Martel M, Hincke MT (2014) Antimicrobial histones from chicken erythrocytes bind bacterial cell wall lipopolysaccharides and lipoteichoic acids. Int J Antimicrob Agents 44:470–472
Rose-Martel M, Kulshreshtha G, Berhane NA, Jodoin J, Hincke MT (2017) Histones from avian erythrocytes exhibit antibiofilm activity against methicillin-sensitive and methicillin-resistant *Staphylococcus aureus*. Sci Rep 7:45980
Sathyan N, Philip R, Chaithanya ER, Anil Kumar PR (2012a) Identification and molecular characterization of molluskin, a histone-H2A-derived antimicrobial peptide from molluscs. ISRN Mol Biol 2012:219656
Sathyan N, Philip R, Chaithanya ER, Kumar PA, Antony SP (2012b) Identification of a histone derived, putative antimicrobial peptide Himanturin from round whip ray *Himantura pastinacoides* and its phylogenetic significance. Results Immunol 2:20–124
Sathyan N, Philip R, Chaithanya ER, AnilKumar PR, Sanjeevan VN, Singh IS (2013) Characterization of Histone H2A derived antimicrobial peptides, Harriottins, from Sicklefin Chimaera *Neoharriotta pinnata* (Schnakenbeck, 1931) and its evolutionary divergence with respect to CO1 and Histone H2A. ISRN Mol Biol. https://doi.org/10.1155/2013/930216
Sharma A, Gupta P, Kumar R, Bhardwaj A (2016) dPABBs: a novel in silico approach for predicting and designing anti-biofilm peptides. Sci Rep 6:21839
Spill F, Guerrero P, Alarcón T, Maini PK, Byrne HM (2015) Mesoscopic and continuum modelling of angiogenesis. J Math Biol 70:485–532
Sruthy KS, Nair A, Antony SP, Puthumana J, Singh IB, Philip R (2019) A histone H2A derived antimicrobial peptide, Fi-Histin from the Indian White shrimp, *Fenneropenaeus indicus*: molecular and functional characterization. Fish Shellfish Immun 92:667–679
Tagai C, Morita S, Shiraishi T, Miyaji K, Iwamuro S (2011) Antimicrobial properties of arginine-and lysine-rich histones and involvement of bacterial outer membrane protease T in their differential mode of actions. Peptides 32:2003–2009
Tsao HS, Spinella SA, Lee AT, Elmore DE (2009) Design of novel histone-derived antimicrobial peptides. Peptides 30:2168–2173
Yi GS, Park CB, Kim SC, Cheong C (1996) Solution structure of an antimicrobial peptide buforin II. FEBS Lett 398:87–90